Thermoelastic Contact Model to Predict the Behavior of a nominally Smooth Convex Punch Using Fractal

By

Sayel M. Fayyad

Supervisor

Osama Abuzeid

Thesis (M. Sc. in Mechanical Engineering)

2003

www.manaraa.com

1. INTRODUCTION

The determination of specific pressure and deformation in the contact zone is one of the basic problems in the theory of elasticity. The basic solution of contact problems was proposed by Hertz, who assumed that the surface of contacting solids are topographically smooth. Consequently the contact among solids is continuous within the nominal contact area and absent outside. This assumption excludes from consideration all real solids among which the contact is discontinuous and the real area of contact is a small fraction of the nominal contact area.

When a compressive load is applied between a punch and a flat surface, the presence of surface roughness produces imperfect contact at the interface. Such contact is characterized by a large number of contact spots of various sizes spread over the whole contact interface. The degree of imperfect contact is measured by both the size of distributions of these contact spots as well as the actual area of contact, which is a fraction of the apparent or nominal surface area. The prediction of the degree of contact is of great importance to several engineering problems such as power transmission systems, belts-pulleys, gears, friction, wear, thermal and electrical contact resistance (see appendix A).

The topography of rough surfaces strongly influences the contact between two surfaces. Roughness measurement on a variety of surfaces has shown that their structure follows a fractal geometry whereby similar images of the surface appear under repeated magnification. Such a structure is characterized by the fractal dimension D, which lies between 2 and 3 for a surface and between 1 and 2 for a surface profile.

The contact model proposed by Borodich and Mosolov (1992) adapted as a base of this study. However the effect of the temperature on the force-deformation

All Rights Reserved - Library of University of Jordan - Center of Thesis Deposit

www.manaraa.com

relationship is not studied in that work. Another study that forms a base for this work made by Abuzeid (2002).

The objective of this work is to incorporate the effect of temperature on the convex punch model proposed by Borodich and Mosolov (1992). A novel analytical thermo-elastic force-deformation relationship of a nominally convex surface is proposed. The surface will be considered as a cylindrical surface and its roughness will be modeled utilizing the fractal geometry.

A power law relationship between the force applied and the approach is determined using fractal geometry analysis and Cantor structure.

Chapter two gives a literature review for recent studies related to the problem of contact stress and different models of contact. Chapter three an introduction to contact stresses and thermoelasticity concept will be discussed.

Chapter four deals with fractal geometry and the definition of fractal geometry, Cantor set, fractal dimension, self-similarity, self-affinity and some other characteristics of fractal geometry. Chapter five summerizes the flat punch model introduced by Abuzeid (2002) which demonestrates the contact model for flat punch and the effect of bulk temperature. Chapter six discusses the rough convex punch model using fractal geometry and gives the final relationship between the applied force and the approach of the two surfaces taking into account the effect of bulk temperature.

Results are discussed in chapter seven, for different cases of fractal dimension and some other parameters. Chapter eight presents the conclusions and the recommendations of this research.

All Rights Reserved - Library of University of Jordan - Center of Thesis Deposit

www.manaraa.com

2. LITRATURE SURVEY

The closed form solution to the contact problem was first proposed by Hertz (1892). The term Hertzian contact is often encountered in contact problems. Elastic contact stress problems are classified as Hertzian if they satisfy some conditions like:

(1) The bodies are homogeneous, isotropic, obay Hooke's law and experience small strains and rotations.

(2) The contacting surfaces are frictionless.

(3) The dimensions of the deformed contact path remain small compared to the principal radii of the undeformed surfaces.

(4) The deformations are related to the stresses in the contact zones and are predicted by the linear theory of elasticity for half spaces.

(5) The contacting surfaces are continuous.

Early studies of the contact of rough surfaces are described in Archard (1957), Bowden and Tabor (1951, 964). The analysis of the effect of roughness on the contact interaction parameters has attracted wide attension. One of the key studies in this field was conducted by Greenwood and Williamson (1966), where the rough surface was modeled by an identical spherical asperities with either exponential or Ganssian (normal) height distribution. This model is based on the following assumptions:

1. The rough surface is isortopic and nominally flat i.e. the surface topography is stationary and it could be described in terms of three parameters σ', σ'' and σ''' .
2. The asperities are spherical near their summits .
3. The interfacial contact conditions are based on spatial density of asperities of constant radius of curvature lying on Gaussian distribution of summit heights.

All Rights Reserved - Library of University of Jordan - Center of Thesis Deposit

www.manaraa.com

4. The individual asperities are dispersed and the forces acting through neighabering asperities do not influence each other
5. The asperities deform only during contact, i.e. there is no bulk deformation.
6. The reference plane is assumed to be in the mean line position.

Greenwood and Tripp (1967) studied the elastic contact of rough spheres. A review of experimental work for the contact of rough surfaces was made by Woo and Thomas (1980). More studies were presented by Johnson (1985). These studies concluded that rough surfaces are very difficult if not impossible to create and so that surface topography is not a stationary random process and the surface parameters are related to the length of the sample. Tripp (1985) studied the Hertzian contact in two and three dimension. More recent studies was made by Liu et al. (1986), where fractal surface is constructed using the Cantor set, which is used to simulate the electrical contact properties of a rough surface interface . Chang et al.(1987) modified the original Greenwood and Williamson (1966) model to incorporate the effect of the volume conservation when asperity deforms both elastically and plastically. Several other theories of friction, wear, and lubrication based on the Greenwood and Williamson (1966) model were developed and discussed by Bhushan (1990). Handzel et. al (1991) made an experimental verification of the Greenwood-Williamson model for the contact of rough surfaces. However, as pointed out by Majumdar and Bhushan (1991), Majumdar et al.(1991) and Bhushan and Majumdar (1992). A new model was developed by these studies using the Weierstrass-Mandelbrot function ,as discribed by Mandelbrot (1982), to simulate surface roughness. Borodich and Mosolov (1992) invistigated the contact of a nominal flat punch using fractal geometry. The shapes of the punches were described as the Cantor-step functions and the elastic half-space was replaced by

All Rights Reserved - Library of University of Jordan - Center of Thesis Deposit

www.manaraa.com

a linear Winkler foundations. An asymptotic power law which associate the force operating on the punch and the depth of indentation have been obtained, using Hill's solution (Hill,1950) for a punch in contact with a rigid perfectly plastic half space to estimate plastic deformation .

An elastic-perfectly plastic contact of rough surfaces based on the Cantor set was modified by Warren and Krajcinovic (1994). Warren et al. (1996) studied a fractal model for the rigid-perfectly plastic contact of rough surface, where an asymptotic model was proposed, where the geomerty of the rough surface is assumed to be fractal. The rough self-affine fractal structure of the effective surfce is approximated using a deterministic Cantor set representation. Bhushan (1996) studied the contact mechanisms of rough surfaces in tribology single asperity contact. He also used an analytical method or solutions primarily for elastic solids and finite element solutions, primarily for elastic-plastic problems and layered solids.

Yan and Kmovoipoulos (1998) studied the contact of 3D elastic plastic fractal surfaces. The main objectives of their study were to introduce acomprehensive analysis of elastic-plastic rough surfaces and to present numerical results revealing the variation of the interfacial contact force and real contact area during the quasi-static surface approach, in this study also closed form solutions for the elastic and plastic components of the total normal force and real contact area are derived in terms of fractal parameters, material properties, and mean surface separation distance. Abuzeid (2002) studied the flat rough punch model and developed a relation between the force applied and approach taking into account the effect of bulk temperature. Abuzeid (2002) studied a thermo-visco-elastic creep model for the contact of nominal flat surfaces based on fractal geometry .

All Rights Reserved - Library of University of Jordan - Center of Thesis Deposit

www.manaraa.com

The contact model proposed by Borodich and Mosolov (1992) put a primitive formula to treat the convex punch in contact, without taking into account the effect of temperature. This study represents the main refrence for the present work which will takes into account a new parameter, that is the effect of bulk temperature.

All Rights Reserved - Library of University of Jordan - Center of Thesis Deposit

www.manaraa.com

3. THE CONTACT PROBLEM

Introduction

When two bodies not mechanically Joined touch each other without becoming rigidly connected, it is said that they are in contact. They can come into contact either at a point or along a line or over a surface or a combination. Contact stresses are caused by the pressure of one solid body on another over limited areas of contact. In some cases, the contact stresses are experinced when two surfaces are pressed together by an external loads. Contact stresses may be considered the major cause of failure of one body or both contacting bodies. The contact region transmits the forces from one body to the other by means of compressive and tangential or shear stresses if friction is presented. Contact-stress problems arise in the contact of wheel and a rail, in automotive valve cams and tappets …… etc. Typical failures are seen as cracks, pits or flaking in the surface of the material. (There are two cases of contact, first contacting of spheres, second contacting of cylinders). Fig (3.1), illustrates the case two cylinders in contact. The area of contact is a narrow rectangle of width *2b* and length *L*, and the pressure distribution is elliptical.

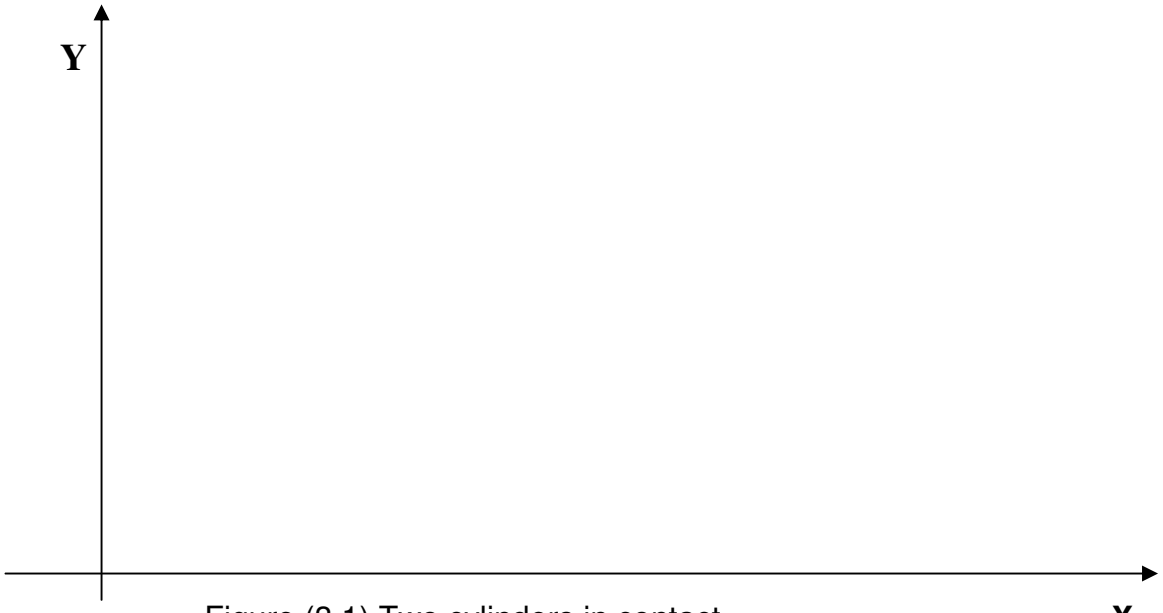

Figure (3.1) Two cylinders in contact.

All Rights Reserved - Library of University of Jordan - Center of Thesis Deposit

www.manaraa.com

For the contacting of cylinders (Figure (3.1)) the maximum pressure is given by:

$$p_{max} = \frac{2p}{\pi bL} \quad (3.1)$$

where:

F: force applied, *b*: width of contact area and *L* is the length of the contact area, and δ represents the approach.

As an example, contact stresses may be significant at the area:-

- Between a locomotive wheel and the railroad.
- Between a roller or a ball and its race in a roller or ball bearings
- Between the teeth of a pair of gears in mesh.
- Between the cam and valve tappets of a gasoline engine. … etc.

Contact stresses are often cyclic in nature and are repeated for a very large number of times, often resulting in a fatigue failure that starts as a localized fracture (crack) associated with localized stresses.

The fact that contact stresses frequently lead to fatigue failure largely explains why these stresses may limit the load carrying capacity in the members in contact and hence may be the significant stresses in the bodies. For more explanation let us take an example of a railroad failure. Sometime it fails as a result of contact stresses, the failure starts as a localized fracture in the form of a minute transverse crack at a point in the head of the rail some where beneath the surface of contact between the rail and the wheel, and progresses outwardly under the influnce of the repeated wheel loads until the entire rail fractures. This fracture is called a transverse fissure failure.

All Rights Reserved - Library of University of Jordan - Center of Thesis Deposit

www.manaraa.com

The principal stresses at or on the contact area between the two curved surfaces that are pressed together are greater than any point beneath the contact area, while the maximum shearing stresses are usually take place at a small distance beneath the contact surface .

Several investigations have attempted to solve this problem. H. Hertz (1892) was the first to obtain a satisfactory solution although his solution gives only the principal stresses in the contact area without any consideration to roughness of the bodies in contact. This solution was considered the basic solution to the problem of mechanical contact among elastically deforming solids.

3.1 Bulk Tempreture Effect:

An isotropic solid element will expand uniformly in all directions when there is an increase in temperature. Thus a sphere will remain a sphere but will undergo a change in radius.This means that there will be an equal normal strain in all directions but no shear strain is noticed for the unconstrained element whose temperature is changed, or if the element is subjected to a hydrostatic stresses, on the other hand, if only a part of the total expansion of the element is permitted, there can be a general state of strain and a general state of stress in the element dependeing on the nature of the constraint.

In an isotropic body subject to a nonuniform temperature distribution, the elements attempt to undergo dilatation or shrinkage as a result of the changes in temperature from some initialy uniform temperature. However, the elements cannot dilate or shrink in an unrestricted manner. Since the body must remain continuous during the change in temperature, there will be partial constraints as to change in geometry. We may then introduce in this way a general stress field in the body. This

All Rights Reserved - Library of University of Jordan - Center of Thesis Deposit

www.manaraa.com

stress field is called thermal stress. High-Speed aircraft and space vehicles are subject to considerable thermal stresses from aerodynamic heating on the out side surfaces and from the heat originating in propulsion systems. Another example appears in the operation of spot welding between the electrods in contact.

To measure the strain developed in a body when it is subject to a temperature field, we superpose the strain associated with free dilatation of the element with the strain associated with the total actual state of strains of the element. This strain includes the thermally induced strain as well as strain due to external loads, or in mathematical expression the strain at a point of a body is given by

$$\varepsilon = \varepsilon' + \varepsilon'' + \varepsilon''' \qquad (3.2)$$

where

ε: is total strain of a body

ε′: is strain from free expansion or shrinkage.

ε″: is strain from thermal induced stress.

ε‴: is strain due to external loads.

For a small temperature change ΔT the change in length of a vanishingly small line segment δL is :

$$\Delta(\delta L) = \alpha \delta L \Delta T \qquad (3.3)$$

Where α is the coefficient of linear thermal expansion. The effect of bulk temperature ΔT in tensile or compression forces can be represented by the formula:

$$P = E \alpha A \Delta T \qquad (3.4)$$

Where:

E: is modulus of elasticity (Pa).

All Rights Reserved - Library of University of Jordan - Center of Thesis Deposit

www.manaraa.com

A: is the cross sectional area (m^2). Thus the thermal stress in the body can be written as:

$$\sigma = \frac{P}{A} = E\alpha\Delta T \tag{3.5}$$

3.2 The Effect of Roughness in Contact Problems

The influnce of surface roughness on contact behaviour is of great importance in many tribological situations. In the last decade several methods have described how to calculate the pressure distribution and the real contact area in contacts between rough surfaces. A problem arising for most contact types is that the size of the contact is much greater than the size of the asperities. Accordingly the number of contact nodes necessary for an accurate solution to the problem becomes excessively large. It is well known that surface roughness has a significant effect on how loads are transmitted at the contact interface between solid bodies. Surface roughness causes high local pressures (in the same order of magnitude as the Vickers hardness) and decreases significantly the real contact area compared to the corresponding smooth case.

Apart from causing high contact stresses the surface roughness is crucial with respect to wear, friction and lubrication properties of the contact. Since the costs are significantly higher when smooth surfaces are manufactured, it is important to understand how surface roughness affects the contact conditions and to be able to predict an acceptable degree of roughness for specific contact situations, Stefan(2001).

All Rights Reserved - Library of University of Jordan - Center of Thesis Deposit

www.manaraa.com

3.3 Winkler Foundations

It is a continous elastic foundations, which presumes a linear force –deflection relationship, so that if a deflection *w* is imposed on the foundation, it resists with a pressure *kw* where k is the foundation modulus. A Winkler foundation deflects only where there is load (see fig, 3.2,a,b). Adjacent material is utterly unaffected. One might expect that an elastic solid would be a more accurate foundation model for soil. This does not seem to be so because soil tends to exhibit a nonlinear response . Of the two models the Winkler model is far easier to analyze. Experience has shown the Winkler model to be adequte for various problems : the railroad rail, piers supported by biling and loaded by horizental force, networks of beams in a floor systems, highway slabs and structures that float, Robert(1985) .

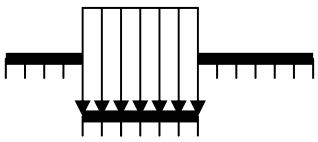

Figure (3.2a) Winkler foundation.

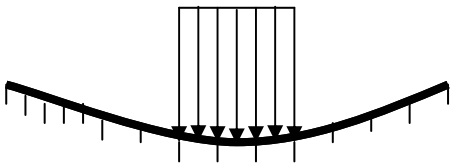

Figure(3.2b) Elastic solid foundation

All Rights Reserved - Library of University of Jordan - Center of Thesis Deposit

www.manaraa.com

4. INTRODUCTION TO FRACTAL GEOMETRY

Introduction

It is of importance to begin with this question: how long is the contour length along a straight line on an engineering surface? At first this qustion may seem trivial. Given a surface profile one can sit down with a ruler and soon come up with a value for the length.

The problem is that: repeating the operation with decreasing the unit of the measured length does not converge but, instead, increase monotically.

Mondelbrot(1982) proposed the idea of a fractel as a way to cope with problems of scale in the real world. He defined the fractal to be any curve or surface that is independnt of scale. This property, referred to as self-similarity or self-affinity, means that any portion of the curve if blown up in scale would appear identical to the whole curve.

4.1 Housdroff – Besicovitch Dimension:

From mathematical point of view, fractal is usually defined as a set for which the Housdroff-Besicoritch dimension exceeds the topological dimension. The dimension D_{HB} of a *(HB)* set *S* is defined as the critical dimension at which the d-

All Rights Reserved - Library of University of Jordan - Center of Thesis Deposit

www.manaraa.com

dimensional measure $M_d(U)$ of a set U(d-dimension of covering U) changes from zero to infinity(see chapter five), and it can be written as:

$$M_d(U) \propto N(\delta)\ \delta^d \Big|_{\delta \to o} \begin{cases} 0, & d > D_{HB} \\ \infty, & d < D_{HB} \end{cases} \tag{4.1}$$

where, $N(\delta)$: is the number of sets of size δ that cover U, and d is the dimension of the object if it makes the measure $M_d(U)$ independent of the unit of measurment δ in the limit of $\delta \to \infty$.

Fractal dimension provides a way to measure how rough fractal curves are, it follows from equation (4.1) that the dimension D_{HB} can be defined as:

$$D_{HB} = \lim_{\delta \to o}\ \inf\ \frac{\ln N(\delta)}{\ln(1/\delta)} \tag{4.2}$$

where (lim inf) defines the infierior limit.

From the definition of fractal, it follows that as the characteristic size *"δ"* tends to zero, the characteristic linear measure of the fractal tends to infinity.

As stated before locally invariant under scalar (Similarity) fractal structure are transformation, and for a stochastic fractal, all directions are equally likely and the extension factor is the same for all coordinates. This is quite acceptable for describing structures that are formed under isotropic conditions, but if the fractal structures form where is a ppreciable an isotropy of properties or processes, isotropic behavior during a scalar transformation can no longer be eccepted. However, an attempt can still be made to keep the basic idea of the fractal approach, associated with scalling of the structure during scalar transformation, using a group of self-affine scalar transformatoin, instead of the self-similar extension with respect to all the coordinates.

All Rights Reserved - Library of University of Jordan - Center of Thesis Deposit

www.manaraa.com

4.2 Self Similarity and Self-Affinity

- **Self Similarity**: when a piece of a shape is geometrically similar to the whole, both the shape and the generating mechanism that generate it are called self-similar. In other words, in an Euclidean space of a dimension "*n*" a real ratio *"$\delta>0$"* determines a transformation called similarity. It transforms the point *"$x=(x_1 \ldots x_2 \ldots x_m \ldots x_n)$"* into the point *"$\delta(x)=(\delta x_1 \ldots \delta x_2 \ldots \delta x_m \ldots \delta x_n)$"*, and hence transforms a set "*S*" into the set *"$\delta(S)$"*.
- **Self Affinity:** The impotant concept of self-affine fractals, which are locally invariant can be defined in the following way: in an Euclidean space of dimension "*n*", a collection of a positive real ratio *"$\delta=(\delta_1 \ldots \delta_2 \ldots \delta_m \ldots \delta_n)$"* determine affinity. It transforms each point "$X=(x_1 \ldots x_m \ldots x_n)=(\delta x_1 \ldots \delta x_m \ldots \delta x_n)$ hence transforms a set *"S"* into the set *"$\delta(S)$"*.

4.3 Mathmatical models :

To explain the idea of the fractal and fractal characteristics of a rough surface let us take the fractional Brownian motion (fBm):

$B_H(X)$ represents one of the most useful mathematical models which examine self-affine fractal structure. In the one-dimensional case $B_H(X)$ is a single-valued random function of the variable X, such that the increment $(B_H(X_2)-B_H(X_1))$ has a Gaussion distribution with variance:

$$\left\langle \left| B_H(X_2) - B_H(X_1) \right|^2 \right\rangle \propto \left| X_2 - X_1 \right|^{2H}, \quad 0 < H < 1, \tag{4.3}$$

All Rights Reserved - Library of University of Jordan - Center of Thesis Deposit

www.manaraa.com

where ⟨ ⟩ denotes averaging over the ensemble, Brownian motion is a special case of this function when "$H = \frac{1}{2}$". The relation between fractal dimension *D*, *H* parameter (Hurst index) and Euclidean dimension'n' can be written as:

$$D=n+1-H \tag{4.4}$$

Brownian motion function is essential in studying rough surfaces because the profiles of rough surfaces are self-affine and follow the statistics of equation (4.3). In this case for trajectories of (fBm), it canbe shown that**:**

$$\Delta B_H \propto \Delta X^H \tag{4.5}$$

The scaling behavior of the different traces is characterized by a particular *H* that relates the typical change in $\Delta z(x)$ to change in the spatial coordinate Δx by the simple scaling law as:

$$\Delta z(x) \propto \Delta x^H \tag{4.6}$$

where $H=2-D$

4.4 Cantor Set.

A very simple construction due to Cantor generates fractal sets with a fractal dimension in the range $0 < D_c < 1$. See fig (4.1) the initiator is the unit interval [0,1], and the generator divides the interval into three equal parts and deletes the open middle part leaving its end points.

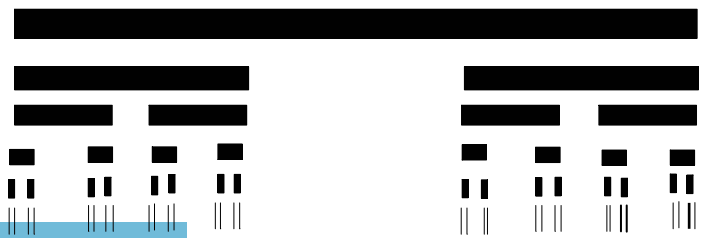

All Rights Reserved - Library of University of Jordan - Center of Thesis Deposit

www.manaraa.com

Figure (4.1) Construction of the triadic Cantor dust.

The generator is then applied again to each of the two parts and so on. This procedure very quickly produces extremely short segments. Because of the resolution of our graphics we find that already the 6-th generation cannot be distinguished from the 5-th generation. After an infinite number of generations what remains is an infinite number of points scattered over the interval. This set is called the Cantor dust Madelbrot (1982).

To evaluate the various dimensions for different forms of the Cantor set, let us consider the Housdroff-Besicovitch dimension defined by equation (4.1).

In the i*th* generation we have $N = 2^i$ segments, each of length :

$$L_i = 3^{-i} \quad \text{, For i = 1,2,....} \tag{4.7}$$

from equation (4.7), to cover the set with line segments of length $\delta = L_i$ and place them carefully we may cover all segments generated in the i*th* generation and, therefore, all points in the Cantor set. Then we can rewrite aquation (4.1) as

$$M_d = \sum_{i=1}^{N} \delta^d = 2^i \left(\frac{1}{3}\right)^{id} = \delta^{d-D} \tag{4.8}$$

This measure tends to zero as δ is decreased, unless we choose $d = D_c = \frac{\ln 2}{\ln 3}. =$ 0.6309. The topological dimension of the Cantor set is $D_{TC} = 0$, as $D_{TC} < D_c$, we

All Rights Reserved - Library of University of Jordan - Center of Thesis Deposit

www.manaraa.com

conclude that the middle third (Triadic) Cantor set is a fractal set with a fractal dimension D_c.

All Rights Reserved - Library of University of Jordan - Center of Thesis Deposit

www.manaraa.com

5. FLAT PUNCH MODELS

Introduction:

In this model we select a surface built on the basis of a regular fractal and analyze the contact problem for the surface, assuming that the results hold for all problems with surfaces of the same fractal dimension. Possibly the simplest model of a polished fractal surface is based on a deterministic fractal; the middle third Cantor set. The Cantor structure is constructed by joining the segments obtained at successive stages of the construction of a Cantor set to one another, Figure (5.1) and figure (5.2). At each stage of construction, the middle section of each initial segment is discarded so that the total length of the remaining segments is *(1/*a*)* times the length of the initial segment, where *(*a*>1)*. The depth of the recesses (measured from the last step) at the (i+1)*th* construction step of the fractal surface is *(1/b)* times less than the depth of the ith step, where *(b>1)*. From this it can easily be shown that the horizontal length and recess depth of the (i+1)*th* step are, respectively:

$$L_{i+1} = a^{-1} L_i = a^{-(i+1)} L_0, \quad (5.1)$$

$$h_{i+1} = b^{-1} h_i = b^{-(i+1)} h_0, \quad (5.2)$$

in which the surface is assumed to be smooth in a direction perpendicular to the plane of the page, i.e. isotropic fractal. This restriction is not very important because it is possible to construct a fractal Cantor surface perpendicular to the plane of the page, Borodich and Mosolov (1992). To see under what conditions the surface constructed is itself a fractal, the length of the constructed contour could be determined. After i iteration, the length is equal:

$$L_i = L_0 + 2h_0 (2b^{-(i+1)}-1) / (2b^{-1}-1) \quad (5.3)$$

All Rights Reserved - Library of University of Jordan - Center of Thesis Deposit

www.manaraa.com

It is obvious that only for $b \leq 2$ the contour of the surface of the structure will be a fractal, because in this case the length L_i tends to an infinite limit.

Using Cantor construction shown in Fig(5.1) below and by referring to equation (4.2) we obtain the dimension of the section of a Cantor set:

$$D_c = \frac{\ln N(\delta)}{\ln(1/\delta)} = \frac{\ln 2}{\ln 2a} \tag{5.4}$$

Also, using equation (5.3) and (5.4), we can obtain the fractal dimension as:

$$D_F = 1 + \frac{\ln(2)}{\ln(2a)} - \frac{\ln(b)}{\ln(2a)} = 1 + D_c - \frac{\ln(b)}{\ln(2a)} \leq 2 \tag{5.5}$$

Also, for the problem of the indentation of a fractal punch in the elastic formulation, when an elastic half-space is covered by a thin elastic layer of equal or lower rigidity in a number of cases the thin covering can operate like a layer of Winkler springs, with the elastic base operating like a continuous set of vertical elastic rods or springs Abuzeid (2002). To examine the indentation of a fractal punch by using Winkler base of depth (bh_0):

$$\Delta F_{i+1} = F_i - F_{i+1} = L_i \, \Delta u_{i+1} \tag{5.6a}$$

$$\frac{\Delta F_{i+1}}{\Delta u_{i+1}} = E(bh)^{-1} L_0 a^{-i} \tag{5.6b}$$

and we can find the force F as $i \to \infty$ as:

$$F = \frac{E h_0 L_0}{b h_o (1+\chi)} \left(\frac{u}{h_0} \right)^{\gamma} \tag{5.6c}$$

and

$$\gamma = \frac{2 - D_F}{1 + D_c - D_F}, \qquad 1 < \gamma < 2 \tag{5.6d}$$

where:

All Rights Reserved - Library of University of Jordan - Center of Thesis Deposit

www.manaraa.com

i: is number of iteration, and $\chi = \frac{\ln a}{\ln b}$.

The profile of the surface Figure in (5.1) can be considered as a certain graph of step function. It can be seen that with scaling $\Delta x_{i+1}=(2a)^{-1}\Delta x_i$ corresponding to an iterational step in constructing the surface, fluctuation Δz of z behaves as $\Delta z_{i+1}=(a\ b)^{-1}\Delta z_i$. In fact, at the i*th* iteration step $\Delta z_i \propto z_i P(z_i)$, where $P(z_i)$ is the probability of obtaining the value z_i, $z_i=h_0/b^i$, $p(z_i)=(1-a^{-1})a^{-i}$. Putting $\Delta z(x) \propto \Delta x^H$, we find $(2a)^H=a\ b$. This gives:

$$H = \frac{\ln(ab)}{\ln(2a)} \tag{5.7}$$

from which the self-affine fractal dimension for the contour of the Cantor structure is derived as:

$$D = 2-H \tag{5.8}$$

All Rights Reserved - Library of University of Jordan - Center of Thesis Deposit

www.manaraa.com

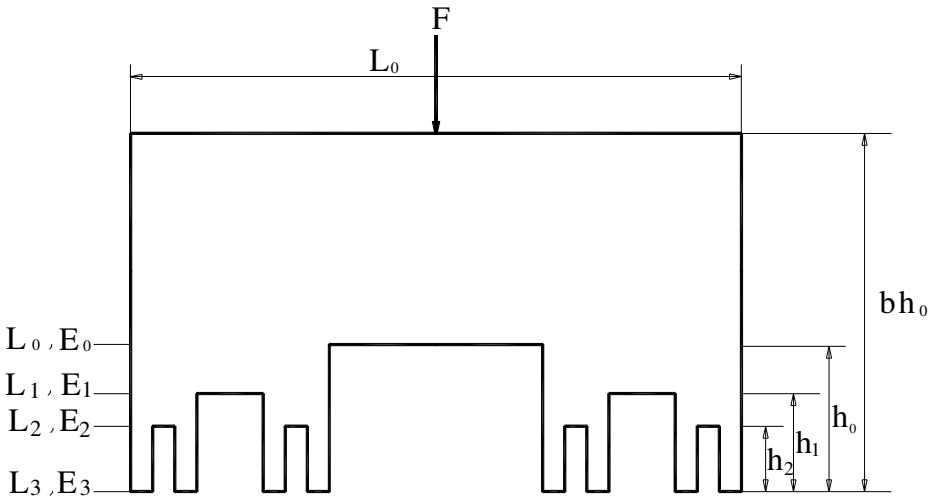

Figure (5.1) Cantor structure with s=2, D_c=0.63093.

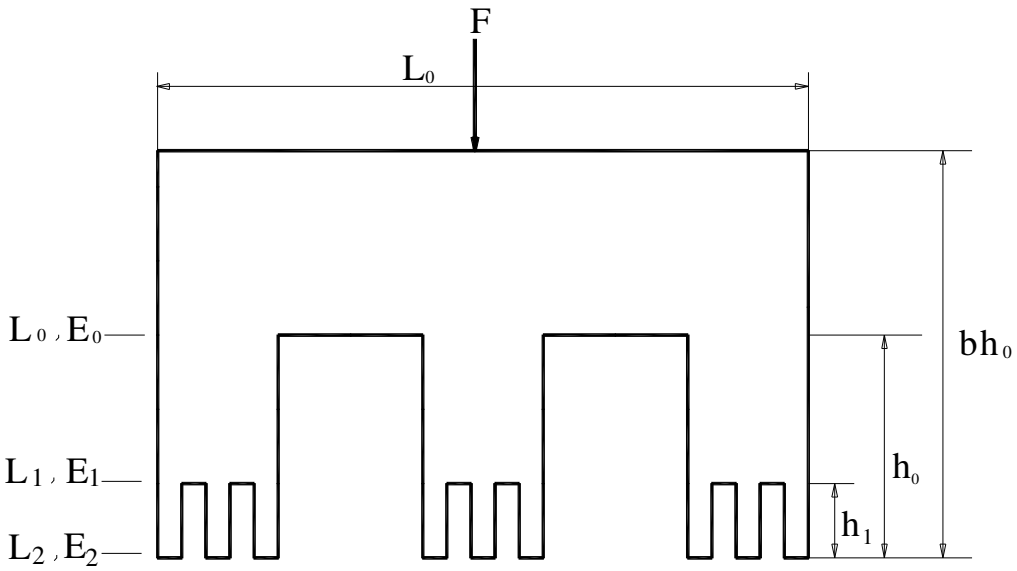

Figure (5.1) Cantor structure with s=3, D_c=0.6228.

All Rights Reserved - Library of University of Jordan - Center of Thesis Deposit

www.manaraa.com

5.1 The Discrete Thermo-Elastic Model

In this model the asperities act like a compliant layer on the surface of the body, so that contact is extended over a larger area than it would be if the surface were smooth, and so all the deformation process is limited in a surface layer which represents all the asperities; bh_0 in Fig (5.1) and their deformation is assumed to be elastic.

The yield strength σ_y, the modulus of elasticity E, and coefficient of thermal expansion α are assumed to be independent of temperature. While this assumption limit the applicability of the solution obtained to certain ranges of temperatures, it makes it possible to investigate a large class of engineering problems. The problem is assumed to be a steady state problem, i.e. temperature is independent of time and there is no heat generation in the body.

Quantitatively we will assume, with reference to Fig (5.1), that there exists a series of springs or elastic bars distributed in a way such that, the distance from the initiator step E_0 to the generates step E_3 is indicated by h_0, from $E_1$to E_3 by h_1, from E_2 to E_3 by h_2, etc. Abuzeid (2002). Let F_3 be the force required to compress E_3 until E_2, F_2 be the force require to compress E_3 and E_2 until E_1, and F_1 be the force required to comprress E_3, E_2 and E_1 until E_0, the remote forces effect can be written as:

$$F_3 = h_2\, k_3 \tag{5.9a}$$

$$F_2 = (h_1 - h_2)\, k_2 + h_1\, k_3 \tag{5.9b}$$

$$F_1 = (h_0 - h_1)\, k_1 + (h_0 - h_2)\, k_2 + h_0\, k_3 \tag{5.9c}$$

And for the bulk temperature effect as:

$$F_3 = E\alpha\Delta T\, L_3, \tag{5.10a}$$

$$F_2 = E\alpha\Delta T\, (L_3 + L_2) \tag{5.10b}$$

All Rights Reserved - Library of University of Jordan - Center of Thesis Deposit

www.manaraa.com

$F_1 = E\alpha\Delta T\,(L_3 + L_2 + L_1)$ (5.10c)

Where $k_i = EL_i / bh_0$ is the stiffness of the i*th* step, E is the modulus of elasticity of the material used, bh_0 could be understood from fig (5.1), and h_i, L_i can be calculated using equation (5.1), and (5.2) respectively.

Let $\Delta F_{i+1}=F_i-F_{i+1}$, assuming unit depth (perpendicular to the plane of the page) we can conclude the general equation for any number of steps as follows:

$$\frac{F_i}{L_0} = F_{i+1} + \frac{E}{b}(b-1)\left(\frac{1}{b}\right)^i \sum_{j=i}^{N}\left(\frac{1}{a}\right)^j - E\alpha\Delta T\left(\frac{1}{a}\right)^i \quad (5.11)$$

where ΔT is the change in the bulk temperature, N is the number of the last step; $N=3$ in Figure (5.1).

5.2 The Continuous Themo-Elastic Model

Since the force in equation (5.11) is derived in the form of sums, it is discrete in nature and it is a discontinuous function of the heights and lengths of the different steps. So it is of interest to derive a continuous solution for the thermo-elastic problem and compare it with that in equation (5.11).

Let F_{i+1} be the limit for protrusion of the (i+1)*th* generation. We will assume that when the limit load is reached, the punch approaches a distance Δu_{i+1}, equal to the difference between the heights protrusion of i*th* and (i+1)*th* generations, i.e.,

$\Delta u_{i+1} = h_0\,(b\text{-}1)\,b^{-i}$ (5.12)

The above mentioned assumptions are sufficient to determine the dependence of the limit load F on the approach u. We will use the fact that the punch is approached by an amount Δu_{i+1} when the limit load increases from F_{i+1} to F_i, we get for the remote load effect:

All Rights Reserved - Library of University of Jordan - Center of Thesis Deposit

www.manaraa.com

$$\frac{\Delta F_{i+1}}{\Delta u_{i+1}} = \frac{EL_0}{bh_0} a^{-i} \tag{5.13}$$

In the limit as $i \rightarrow \infty$, we obtain the following asymptotic behavior:

$$F_R = \frac{EL_0}{bh_0} \frac{h_0}{\chi} \left(\frac{u}{h_0} \right)^{\chi+1} \tag{5.14}$$

Where $\chi = \ln a / \ln b$, and for the bulk temperature effect:

$$\frac{\Delta F_{i+1}}{\Delta u_{i+1}} = \frac{EL_0}{h_0} \frac{\alpha \Delta T}{b-1} \left(\frac{b}{a} \right)^{i} \tag{5.15}$$

In the limit as $i \rightarrow \infty$, we obtain the following asymptotic behavior:

$$F_T = \frac{EL_0}{b-1} \frac{\alpha \Delta T}{\chi} \left(\frac{u}{h_0} \right)^{\chi} \tag{5.16}$$

Then the limit load due to the dual effect could be obtained by summing up equations (5.14) and (5.16). We obtain:

$$\frac{F}{L_0} = \frac{E}{b} \frac{1}{\chi} \left(\frac{u}{h_0} \right)^{\chi+1} - \frac{E}{b-1} \frac{\alpha \Delta T}{\chi} \left(\frac{u}{h_0} \right)^{\chi} \tag{5.17}$$

Note that a limiting load is also imposed to these models; i.e., $F = \sigma_y L_0$.

We will use these models and the preciding relations (in chapter 5) to build a model for the rough convex punch in the next chapter.

All Rights Reserved - Library of University of Jordan - Center of Thesis Deposit

www.manaraa.com

6. CONVEX PUNCH MODELS

Introduction:

It is well known that the parameters of the actual contact zone of real bodies depend closely on the waviness and roughness of the contact surfaces. It stands to reason that the microgeometry of the surfaces of bodies will have a large effect on their contact properties, especially at the initial stage of compression. Various contact problem for flat fractal punches were considered in Borodich and Mosolov (1992), warren and Krajcinovic (1995) and Warren, Majumdar and Krajcinovic(1996) and Abuzaid (2002). The shapes of the punches were described as the Cantor-step functions and the elastic half-space was replaced by a linear Winkler foundation. An asymptotic power law which associate the force operating on the punch and the depth of indenteation have been obtained. But, for convex punches only little work had been done to study this kind of contact stresses. In this work we will develop a new model for a rough convex punch depending on Mosolov, and Borodich (1992) studies and Abuzeid (2002) taking into account the effect of temperature as an extra load.

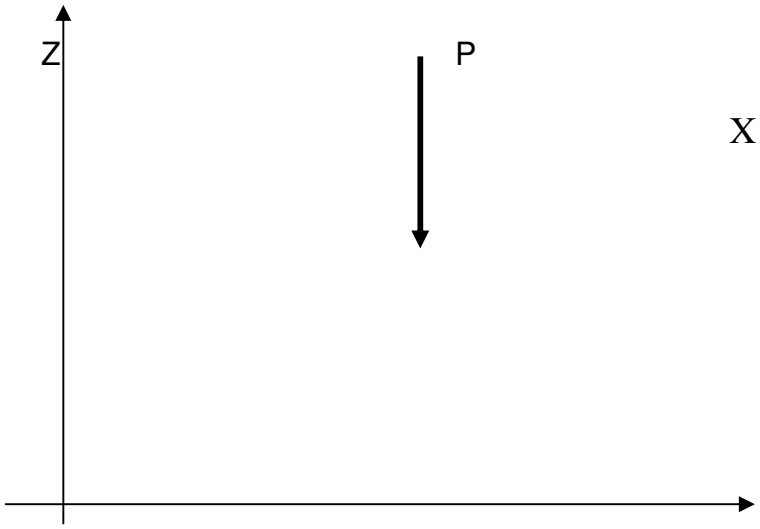

All Rights Reserved - Library of University of Jordan - Center of Thesis Deposit

www.manaraa.com

Figure (6.1) Contact between a cylinderical punch and a rigid flat surface.

6.1 Analysis of Convex Rough Punch Contact Model.

For a convex punch, consider the profile function of the surfase such that Z=*f*(x), Mosolov and Borodich (1992) having a fractal surface. Let (*u)* be the depth of indentation(approach) of the point of the punch under load. It is also assumed that the profile of the punch is symmetrical about the Z-axis. The contact pressure under the punch at any point (of the punch) depends only on its displacement(u). Figure (6.1) shows the convex punch contact model.

The contact force (*P)* along the convex punch is given by the formula of Mosolov and Borodich (1992):

$$P = \int_{o}^{L_*} P(x)dx, \qquad f(L_*) = u \tag{6.1}$$

Where *P*(x) can be given by :

$$P(x) = C[u - f(x)]^{\gamma} \tag{6.2}$$

So we can find the force-displacement relation as:

All Rights Reserved - Library of University of Jordan - Center of Thesis Deposit

www.manaraa.com

$$P=\int_{o}^{L_e} C(u-f(x))^{\gamma}\,dx \tag{6.3}$$

where:

$$C=\frac{Eh_0}{bh_0h_0^{\gamma}(1+\chi)} \tag{6.4}$$

Where:

E: is the modulus of elasticity

h_0 : is the hight of the asprities in Cantor diagram.

bh_0: is the depth of wrinkler base, and $X=\frac{\ln(\ a\ )}{\ln(\ b\ )}$

in general $f(x) = Z = Ax^m$, $A>0,\ m>1$.

But for a convex rough punch we have:

$Z= f(\rho) = A\,\rho^{m}$, $A > 0$, $m > 1$

Where $\rho = \sqrt{x^2+y^2}$

$$\therefore P=C\int_{o}^{L_e}\left(u-A\rho^{m}\right)^{\gamma}d\rho, \text{ A>0, m>1} \tag{6.5}$$

To evaluate this integration using integration tables (Jan Tuma) we find that:

$$\int_{o}^{a} X^{T-1}\left(a^{\mu}-X^{\mu}\right)^{B-1}dX=a^{\mu(B-1)+T}\mu^{-1}\beta\left(\frac{T}{\mu},B\right) \tag{6.6}$$

where a, μ, Re a, Re B > 0

and $\beta\left(\frac{T}{\mu},B\right)$ is the Betta function

but our integration is

$$P=C\int_{o}^{L_e}\left(u-A\rho^{m}\right)^{\gamma}d\rho \tag{6.7}$$

All Rights Reserved - Library of University of Jordan - Center of Thesis Deposit

www.manaraa.com

Using equation (6.6) the integration given in equation (6.7) can be evaluated to give:

$$P = CA^{\frac{1}{\gamma}} \int_{o}^{L_*} \left[\left(\left(\frac{u}{A} \right)^{\frac{1}{m}} \right)^{m} - \rho^{m} \right]^{\gamma} d\rho \qquad (6.8)$$

So we can solve the integration in equation (6.8) to get

$$P = CA^{\frac{1}{\gamma}} {}_{o}\int^{K} \left(K^{m} - \rho^{m} \right)^{\gamma} \, d\rho$$

$$= C A^{\frac{1}{\gamma}} \left[K^{m\gamma+1} m^{-1} \beta\left(\frac{1}{m}, \gamma+1 \right) \right]$$

$$P = CA^{\frac{1}{\gamma}} \left(\frac{u}{A} \right)^{\gamma+\frac{1}{m}} m^{-1} \beta\left(\frac{1}{m}, \gamma+1 \right)$$

$$\therefore P = \frac{C A^{\frac{1}{\gamma}}}{m} \left(\frac{u}{A} \right)^{\gamma+\frac{1}{m}} \beta\left(\frac{1}{m}, \gamma+1 \right) \qquad (6.9)$$

Where

$$\gamma = \frac{2 - D_F}{1 + Dc - D_F} > 1$$

D_F: is the profile dimension.

D_c: Cantor set dimension .

$\beta(\,)$: Betta function which can be defined as

$$\beta(x, y) = {}_{o}\int^{1} t^{x-1} (1-t)^{y-1} dt = \frac{\Gamma(x)\Gamma(y)}{\Gamma(x+y)}$$

where Γ(x) : is gamma function.

As a result we found that :

$$P = \frac{E h_0 A^{\frac{1}{\gamma}}}{h_0^{\gamma} b \, h_0 (1+x) m} \beta\left(\frac{1}{m}, \gamma+1 \right) \left(\frac{u}{A} \right)^{\gamma+\frac{1}{m}} \qquad (6.10)$$

All Rights Reserved - Library of University of Jordan - Center of Thesis Deposit

المنارة للاستشارات
www.manaraa.com

This equation represents the relationship between approach produced by the effect of impressed contact force and the force applied it self. Thus, it has been shown in a specific case that fracted roughness of the surface of contacting bodies gives the well known power laws of the form $p \sim u^{\gamma}$. To put equation (6.10) in a nondimensional form taking the exponent (*m=2, for the cylindrical punch*) we get:

$$\therefore \frac{P}{L_{\max}} = \frac{E}{8b(1+\chi)} \beta(0.5, \gamma+1) \left(\frac{u}{h_0}\right)^{\gamma+0.5} \tag{6.11}$$

where $L_{max}=(2Rh_0)^{0.5}$, R: is the radius of the punch.

6.2 The Continuous Thermo -Elastic Model

A relation between the approach and force under the effect of bulk temperature is to be determined. The bodies treated will be assumed to be isotropic and homogeneous. The yeild strength σ_y and the modulus of elasticity E, and coefficient of thermal expansion α are assumed to be independent of temperature.

Thermal stresses may arise in a heated body because of a non uniform temperature distribution. The problem is also assumed to be a steady state problem, i.e temperature is independent of time and there is no internal(generation) heat in the body, and temperature is assumed to be uniformly incereased by ΔT.

We also can write that (under the effect of bulk temperature):

$$p_T = \int_o^{L_*} P(x)\, dx, \quad f(L_*) = u \tag{6.12}$$

Where :

P(x) can be given by

$$P(x) = C_T [u - f(x)]^{\gamma} \tag{6.13}$$

All Rights Reserved - Library of University of Jordan - Center of Thesis Deposit

www.manaraa.com

Where

$C_T = E\alpha\,\Delta T L_0$

E : Modulus of Elasticity.

α : Thermal Coefficient Expansion and ΔT: bulk Temperature change.

So we can write:

$$P_T = \int_0^{L_e} C_T\left(u - A\rho^n\right)d\rho, \quad A>0, m>1 \tag{6.14}$$

by the integation we get (in a non dimensional form)

$$\frac{P_T}{L_{\max}} = \frac{E\,\alpha\,\Delta T}{2}\left(\frac{u}{h_0}\right)^{\gamma+\frac{1}{2}}\beta\left(\frac{1}{2},\gamma+1\right) \tag{6.15}$$

The total load due to the dual effect could by obtained by summing up eqs (6.11) and (6.15). We obtain:

$$\frac{P}{L_{\max}} = \left[\frac{E}{8\,b\,(1+\chi)}\left(\frac{u}{h_0}\right)^{\gamma+\frac{1}{2}} - \frac{E\,\alpha\,\Delta T}{2}\left(\frac{u}{h_0}\right)^{\gamma+\frac{1}{2}}\right]\beta\left(\frac{1}{2},\gamma+1\right) \tag{6.16}$$

or we can rewrite eqation (6.16)in the form:

$$p^* = \left[\frac{E}{8\,b\,(1+\chi)}\left(u^*\right)^{\gamma+\frac{1}{2}} - \frac{E\,\alpha\,\Delta T}{2}\left(u^*\right)^{\gamma+\frac{1}{2}}\right]\beta\left(\frac{1}{2},\gamma+1\right) \tag{6.17}$$

Equation (6.17) represents the relationship between the force applied and the approach for the convex punch model in a non dimensional form taking into account the effect of the bulk tempreture. Note that a limiting load is also imposed to these models; i.e., $P=\sigma_y L_{max}$.

All Rights Reserved - Library of University of Jordan - Center of Thesis Deposit

www.manaraa.com

All Rights Reserved - Library of University of Jordan - Center of Thesis Deposit

www.manaraa.com

1. INTRODUCTION

The determination of specific pressure and deformation in the contact zone is one of the basic problems in the theory of elasticity. The basic solution of contact problems was proposed by Hertz, who assumed that the surface of contacting solids are topographically smooth. Consequently the contact among solids is continuous within the nominal contact area and absent outside. This assumption excludes from consideration all real solids among which the contact is discontinuous and the real area of contact is a small fraction of the nominal contact area.

When a compressive load is applied between a punch and a flat surface, the presence of surface roughness produces imperfect contact at the interface. Such contact is characterized by a large number of contact spots of various sizes spread over the whole contact interface. The degree of imperfect contact is measured by both the size of distributions of these contact spots as well as the actual area of contact, which is a fraction of the apparent or nominal surface area. The prediction of the degree of contact is of great importance to several engineering problems such as power transmission systems, belts-pulleys, gears, friction, wear, thermal and electrical contact resistance (see appendix A).

The topography of rough surfaces strongly influences the contact between two surfaces. Roughness measurement on a variety of surfaces has shown that their structure follows a fractal geometry whereby similar images of the surface appear under repeated magnification. Such a structure is characterized by the

All Rights Reserved - Library of University of Jordan - Center of Thesis Deposit

www.manaraa.com

fractal dimension D, which lies between 2 and 3 for a surface and between 1 and 2 for a surface profile.

The contact model proposed by Borodich and Mosolov (1992) adapted as a base of this study. However the effect of the temperature on the force-deformation relationship is not studied in that work. Another study that forms a base for this work made by Abuzeid (2002).

The objective of this work is to incorporate the effect of temperature on the convex punch model proposed by Borodich and Mosolov (1992). A novel analytical thermoelastic force-deformation relationship of a nominally convex surface is proposed. The surface will be considered as a cylindrical surface and its roughness will be modeled utilizing the fractal geometry.

A power law relationship between the force applied and the approach is determined using fractal geometry analysis and Cantor structure .

Chapter two gives a literature review for recent studies related to the problem of contact stress and different models of contact. Chapter three an introduction to contact stresses and thermoelasticity concept will be discussed.

Chapter four deals with fractal geometry and the definition of fractal geometry, Cantor set, fractal dimension, self-similarity, self-affinity and some other characteristics of fractal geometry. Chapter five summarizes the flat punch model introduced by Abuzeid (2002) which demonstrates the contact model for flat punch and the effect of bulk temperature. Chapter six discusses the rough convex punch model using fractal geometry and gives the final relationship

All Rights Reserved - Library of University of Jordan - Center of Thesis Deposit

www.manaraa.com

between the applied force and the approach of the two surfaces taking into account the effect of bulk temperature.

Results are discussed in chapter seven, for different cases of fractal dimension and some other parameters. Chapter eight presents the conclusions and the recommendations of this research .

All Rights Reserved - Library of University of Jordan - Center of Thesis Deposit

www.manaraa.com

2. LITRATURE SURVEY

The closed form solution to the contact problem was first proposed by Hertz (1892). The term Hertzian contact is often encountered in contact problems. Elastic contact stress problems are classified as Hertzian if they satisfy some conditions like:

(1) The bodies are homogeneous, isotropic, obey Hook's law and experience small strains and rotations.

(2) The contacting surfaces are frictionless.

(3) The dimensions of the deformed contact path remain small compared to the principal radii of the undeformed surfaces .

(4) The deformations are related to the stresses in the contact zones and are predicted by the linear theory of elasticity for half spaces.

(5) The contacting surfaces are continuous.

Early studies of the contact of rough surfaces are described in Archard (1957), Bowden and Tabor (1951, 964). The analysis of the effect of roughness on the contact interaction parameters has attracted wide attention. One of the key studies in this field was conducted by Greenwood and Williamson (1966), where the rough surface was modeled by an identical spherical asperities with either exponential or Ganssian (normal) height distribution. This model is based on the following assumptions:

All Rights Reserved - Library of University of Jordan - Center of Thesis Deposit

www.manaraa.com

1. The rough surface is isotropic and nominally flat i.e. the surface topography is stationary and it could be described in terms of three parameters σ', σ'' and σ'''.
2. The asperities are spherical near their summits.
3. The interfacial contact conditions are based on spatial density of asperities of constant radius of curvature lying on Gaussian distribution of summit heights.
4. The individual asperities are dispersed and the forces acting through neighboring asperities do not influence each other
5. The asperities deform only during contact, i.e. there is no bulk deformation .
6. The reference plane is assumed to be in the mean line position .

Greenwood and Tripp (1967) studied the elastic contact of rough spheres. Woo and Thomas (1980) made a review of experimental work for the contact of rough surfaces .Johnson (1985) presented more studies. These studies concluded that rough surfaces are very difficult if not impossible to create and so that surface topography is not a stationary random process and the surface parameters are related to the length of the sample. Tripp (1985) studied the Hertzian contact in two and three dimension. More recent studies were made by Liu et.al. (1986), where fractal surface is constructed using the Cantor set, which is used to simulate the electrical contact properties of a rough surface interface. Chang et al.(1987) modified the original Greenwood and Williamson (1966) model to incorporate the effect of the volume conservation when asperity deforms both elastically and plastically. Several other theories of friction, wear, and lubrication based on the Greenwood and

All Rights Reserved - Library of University of Jordan - Center of Thesis Deposit

www.manaraa.com

Williamson (1966) model were developed and discussed by Bhushan (1990). Handzel et. al. (1991) made an experimental verification of the Greenwood-Williamson model for the contact of rough surfaces. However, as pointed out by Majumdar and Bhushan (1991), Majumdar et al. (1991) and Bhushan and Majumdar (1992). A new model was developed by these studies using the Weierstrass-Mandelbrot function, as described by Mandelbrot (1982), to simulate surface roughness. Borodich and Mosolov (1992) investigated the contact of a nominal flat punch using fractal geometry. The shapes of the punches were described as the Cantor-step functions and the elastic half-space was replaced by a linear Winkler foundation. An asymptotic power law which associate the force operating on the punch and the depth of indentation have been obtained, using Hill's solution (Hill, 1950) for a punch in contact with a rigid perfectly plastic half space to estimate plastic deformation.

An elastic-perfectly-plastic contact of rough surfaces based on the Cantor set was modified by Warren and Krajcinovic (1994). Warren et. al. (1996) studied a fractal model for the rigid-perfectly plastic contact of rough surface, where an asymptotic model was proposed, where the geometry of the rough surface is assumed to be fractal. The rough self-affine fractal structure of the effective surface is approximated using a deterministic Cantor set representation. Bhushan (1996) studied the contact mechanisms of rough surfaces in tribology single asperity contact. He also used an analytical method or solutions primarily for elastic solids and finite element solutions, primarily for elastic-plastic problems and layered solids.

All Rights Reserved - Library of University of Jordan - Center of Thesis Deposit

www.manaraa.com

Yan and Kmovoipoulos (1998) studied the contact of 3D elastic plastic fractal surfaces. The main objectives of their study were to introduce a comprehensive analysis of elastic-plastic rough surfaces and to present numerical results revealing the variation of the interfacial contact force and real contact area during the quasi-static surface approach, in this study also closed form solutions for the elastic and plastic components of the total normal force and real contact area are derived in terms of fractal parameters, material properties, and mean surface separation distance. Abuzeid (2002) studied the flat rough punch model and developed a relationship between the force applied and approaches taking into account the effect of bulk temperature. Abuzeid (2002) studied a thermo-visco-elastic creep model for the contact of nominal flat surfaces based on fractal geometry.

The contact model proposed by Borodich and Mosolov (1992) put a primitive formula to treat the convex punch in contact, without taking into account the effect of temperature. This study represents the main reference for the present work which will takes into account a new parameter, that is the effect of bulk temperature.

All Rights Reserved - Library of University of Jordan - Center of Thesis Deposit

www.manaraa.com

3.THE CONTACT PROBLEM

Introduction

When two bodies not mechanically joined touch each other without becoming rigidly connected, it is said that they are in contact. They can come into contact either at a point or along a line or over a surface or a combination. Contact stresses are caused by the pressure of one solid body on another over limited areas of contact. In some cases, the contact stresses are experienced when two surfaces are pressed together by an external load. Contact stresses may be considered the major cause of failure of one body or both contacting bodies. The contact region transmits the forces from one body to the other by means of compressive and tangential or shear stresses if friction is presented. Contact-stress problems arise in the contact of wheel and a rail, in automotive valve cams and tappets … etc. Typical failures are seen as cracks, pits or flaking in the surface of the material. (There are two cases of contact, first contacting of spheres, second contacting of cylinders). Fig (3.1), illustrates the case two cylinders in contact. The area of contact is a narrow rectangle of width *2b* and length *L*, and the pressure distribution is elliptical.

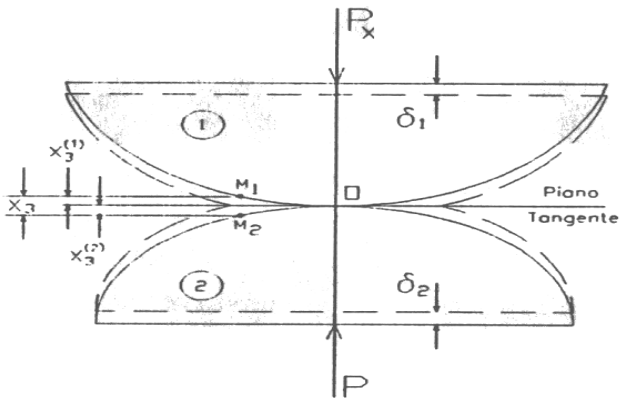

Figure (3.1) Two cylinders in contact

All Rights Reserved - Library of University of Jordan - Center of Thesis Deposit

www.manaraa.com

For the contacting of cylinders (Figure (3.1)) the maximum pressure is given by:

$$p_{max} = \frac{2F}{\pi bL} \quad (3.1)$$

Where:

F: force applied, *b*: width of contact area and *L* is the length of the contact area.

As an example, contact stresses may be significant at the area:-

- Between a locomotive wheel and the railroad .
- Between a roller or a ball and its race in a roller or ball bearings
- Between the teeth of a pair of gears in mesh.
- Between the cam and valve tappets of a gasoline engine … etc.

Contact stresses are often cyclic in nature and are repeated for a very large number of times, often resulting in a fatigue failure that starts as a localized fracture (crack) associated with localized stresses .

The fact that contact stresses frequently lead to fatigue failure largely explains why these stresses may limit the load carrying capacity in the members in contact and hence may be the significant stresses in the bodies. For more explanation let us take an example of a railroad failure. Sometime it fails as a result of contact stresses, the failure starts as a localized fracture in the form of a minute transverse crack at a point in the head of the rail some where beneath the surface of contact between the rail and the wheel, and

All Rights Reserved - Library of University of Jordan - Center of Thesis Deposit

www.manaraa.com

progresses outwardly under the influence of the repeated wheel loads until the entire rail fractures. This fracture is called a transverse fissure failure.

The principal stresses at or on the contact area between the two curved surfaces that are pressed together are greater than any point beneath the contact area, while the maximum shearing stresses are usually take place at a small distance beneath the contact surface.

Several investigations have attempted to solve this problem. H. Hertz (1892) was the first to obtain a satisfactory solution although his solution gives only the principal stresses in the contact area without any consideration to roughness of the bodies in contact. This solution was considered the basic solution to the problem of mechanical contact among elastically deforming solids.

3.1 Bulk Temperature Effect:

An isotropic solid element will expand uniformly in all directions when there is an increase in temperature. Thus a sphere will remain a sphere but will undergo a change in radius.This means that there will be an equal normal strain in all directions but no shear strain is noticed for the unconstrained element whose temperature is changed, or if the element is subjected to a hydrostatic stresses, on the other hand, if only a part of the total expansion of the element is permitted, there can be a general state of strain and a general state of stress in the element depending on the nature of the constraint.

In an isotropic body subject to a non-uniform temperature distribution, the elements attempt to undergo dilatation or shrinkage as a result of the changes in temperature from some initially uniform temperature. However, the

All Rights Reserved - Library of University of Jordan - Center of Thesis Deposit

www.manaraa.com

elements cannot dilate or shrink in an unrestricted manner. Since the body must remain continuous during the change in temperature, there will be partial constraints as to change in geometry. We may then introduce in this way a general stress field in the body. This stress field is called thermal stress. High-Speed aircraft and space vehicles are subject to considerable thermal stresses from aerodynamic heating on the out side surfaces and from the heat originating in propulsion systems. Another example appears in the operation of spot welding between the electrodes in contact.

To measure the strain developed in a body when it is subject to a temperature field, we superpose the strain associated with free dilatation of the element with the strain associated with the total actual state of strains of the element. This strain includes the thermally induced strain as well as strain due to external loads, or in mathematical expression the strain at a point of a body is given by

$$\varepsilon = \varepsilon' + \varepsilon'' + \varepsilon''' \qquad (3.2)$$

Where

ε: is total strain of a body

ε': is strain from free expansion or shrinkage.

ε'': is strain from thermal induced stress.

ε''': is strain due to external loads.

For a small temperature change ΔT the change in length of a vanishingly small line segment δL is :

$$\Delta(\delta L) = \alpha \delta L \Delta T \qquad (3.3)$$

All Rights Reserved - Library of University of Jordan - Center of Thesis Deposit

www.manaraa.com

Where α is the coefficient of linear thermal expansion. The effect of bulk temperature ΔT in tensile or compression forces can be represented by the formula:

$$P = E\alpha A\Delta T \tag{3.4}$$

Where:

E : is modulus of elasticity (Mpa)

A : is the cross sectional area (m^2).

Thus the thermal stress in the body can be written as:

$$\sigma = \frac{P}{A} = E\alpha\Delta T \tag{3.5}$$

3.2 The Effect of Roughness in Contact Problems

The influence of surface roughness on contact behavior is of great importance in many tribological situations. In the last decade several methods have described how to calculate the pressure distribution and the real contact area in contacts between rough surfaces. A problem arising for most contact types is that the size of the contact is much greater than the size of the asperities. Accordingly the number of contact nodes necessary for an accurate solution to the problem becomes excessively large. It is well known that surface roughness has a significant effect on how loads are transmitted at the contact interface between solid bodies. Surface roughness causes high local pressures (in the same order of magnitude as the Vickers hardness)

All Rights Reserved - Library of University of Jordan - Center of Thesis Deposit

www.manaraa.com

and decreases significantly the real contact area compared to the corresponding smooth case.

Apart from causing high contact stresses the surface roughness is crucial with respect to wear, friction and lubrication properties of the contact. Since the costs are significantly higher when smooth surfaces are manufactured, it is important to understand how surface roughness affects the contact conditions and to be able to predict an acceptable degree of roughness for specific contact situations, Stefan (2001).

3.3 Winkler Foundations

It is a continuos elastic foundations, which presumes a linear force –deflection relationship, so that if a deflection *w* is imposed on the foundation, it resists with a pressure kw where k is the foundation modulus. A Winkler foundation deflects only where there is load (see fig, 3.2, a, b). Adjacent material is utterly unaffected. One might expect that elastic solid would be a more accurate foundation model for soil. This does not seem to be so because soil tends to exhibit a nonlinear response. Of the two models the Winkler model is far easier to analyze. Experience has shown the Winkler model to be adequate for various problems: the railroad rail, piers supported by billing and loaded by horizontal force, networks of beams in a floor systems, highway slabs and structures that float, Robert (1985).

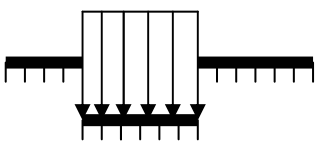

Figure (3.2a) Winkler foundation.

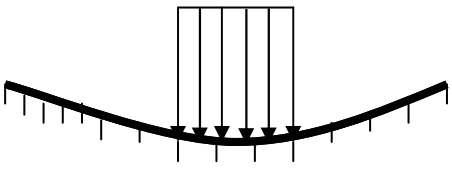

Figure (3.2b) Elastic solid foundation

All Rights Reserved - Library of University of Jordan - Center of Thesis Deposit

www.manaraa.com

7. RESULTS AND DISCUSION

Results

A continuous model for the approach of the Cantor structure of the convex rough punch is already formulated as shown in equation (6.17), it is a new equation that relates the force applied and the approach taking into account the effect of bulk temperature. It is derived depending on fractal geometry and Cantor structure to treat the convex rough punch regardless of the radius of the punch. Values for E, a, b, α, m, and σ_y are required to evaluate equations (6.1) to (6.17), a and b characterize the Cantor structure of the rough punch surface and they are related through the fractal dimension D_f.

The coefficient of thermal expansion for carbon steel is α=10.8x10 $^{-6}$ /° c, the modulus of elasticity E=210 Gpa, and the yield strength is σ =580 Mpa (AISI 1050). Cantor structures shown in figure (5.1), and figure (5.2) are built from the middle third Cantor set. The parameter a =1.5 is held fixed, giving the Cantor dimension D_c=0.63093, and D_c=0.6228 respectively, Mandelbrot (1982), where b =1.115, yield two values of the fractal dimension D_f =1.5and D_f =1.24, are used to study the above mentioned model, also in this model for the cylindrical punch we take m=2 and A=1. To show the effect of the bulk temperature, three different values were used; ΔT=0, ΔT=400 C, and ΔT=800 C. Handzel-Powierza, Klimczak and Polijaniuk(1991) have verified experimentally the contact model developed by Greenwood and Williamson (1967), owing to its simplicity and universality. They conducted their experiments at room temperature, on face turned, ground, and bead-blasted carbon steel specimens (0.45 percent carbon), which were in contact with

All Rights Reserved - Library of University of Jordan - Center of Thesis Deposit

www.manaraa.com

smooth rigid specimen. The error in the experimental measurements was determined to be approximately ±0.5μm for the displacement, and ± 5MPa for the load.

The depth h_0 was taken as 9.7μm, which corresponds to twice root mean square height, obtained by Handzel-Powierza, Klimczak and Polijaniuk (1991), for the bead-blasted surface, and for the turned surfaces we have h_0 to be 40 μm.

Figure (7.1) represents the relation between the force applied and the approach for the case D_f =1.5, D_c=0.63093 at different values of the bulk temperature and we can noticed that we have more approach as the bulk temperature increased, i.e., more approach at ΔT=400 ℃ and ΔT=800 ℃ than at ΔT=0℃. From figure (7.2) which represents the relation between the applied force and the approach for the case D_f =1.24, D_c=0.63093 at different values of bulk temperature. Figure (7.3) represents the relation between the force applied and the approach for the case D_f =1.5, D_c=0.6228 at different values of the bulk temperature.

We can noticed that we have more approach as the bulk temperature increased, i.e. more approach at ΔT=400 ℃ and ΔT=800 ℃ than at ΔT=0℃. Figure (7.4) represents the relation between the applied force and the approach at D_f =1.24, D_c=0.6228 for different values of bulk temperature. Also from figure (7.5) which represents the relation (u* vs. p*) we can notice that more approach can be seen at D_f =1.5 than at D_f =1.24. Figure (7.6) relates the applied force and the approach at D_f =1.5 and ΔT=0℃ at different values of Cantor dimension D_c, we can noticed more deformation at D_c=0.6228 or s=3. Figure (7.7) relates the applied force and the approach at D_f =1.24 and ΔT=0℃

All Rights Reserved - Library of University of Jordan - Center of Thesis Deposit

www.manaraa.com

at different values of Cantor dimension D_c, we can noticed more deformation at D_c=0.6228 or s=3. Figure (7.8) represents the relation between the applied force and the approach and a comparison between the theoretical results and the experimental one for the case of a bead-blasted surface at D_f =1.5, D_c=0.63093 and ΔT=0℃, we can notice a good agreement between the theoretical results and the experimental. In figure (7.9) we can see a good agreement between the theoretical and the experimental results for the case of a bead-blasted surface at D_f =1.5, D_c=0.6228. Figure (7.10) represents the relation (u vs. p) and gives a comparison between the theoretical results and the experimental, for the case of a bead-blasted surface at D_f =1.5, D_c=0.6228, and there is a good agreement between them. In figure (7.11) the agreement between the theoretical and experimental results is not so good for the case of the turned surfaces, at D_f =1.5, D_c=0.63093.

Discussion:

The numerical results generated are presented in a non dimensionalized form ($u^*=u/h_0$) and ($p^*=p/L_{max}$) for the load-displacement relationship in figure (7.1)-figure (7.11) we can deduce the following observations:

1.from figure (7.1) it can be noticed that as the force applied increases approach increases too, and we can see more approach at higher bulk temperature, the relation starts as an elastic relationship between force applied and the approach and then it goes as a plastic deformation. The reason is that as the force applied increases the material deforms more and more until it reaches the plastic state.

All Rights Reserved - Library of University of Jordan - Center of Thesis Deposit

www.manaraa.com

2. From figure (7.1) to figure (7.4) it can be shown that as Cantor dimension decreases I.e. (D_c=0.6228) the difference in approach at different bulk temperature is greater, because the local pressure increases as Cantor dimension increases and the dual effect becomes greater too.

3 .Form figure (7.1)-figure (7.4) more approach can be noticed at the higher bulk temperature i.e. at ΔT=400 ℃ and ΔT=800 ℃, because bulk temperature represents an extra load that cause more deformation .

4. With D_f=1.24, a significantly larger load is required to produce the same approach (u), as with D_f=1.5, Fig. (7.5), the reason behind this is that as the fractal dimension D_f is increased the curve becomes rougher with sharp peaks. Thus higher fractal dimensions give rise to more sharply peaked asperities which plastically deform at lower loads as observed in figures.

6. With D_c=0.63093 more load is required to produce the same approach (u), as with D_c =0.6228, figure (7.6), and figure (7.7) the reason behind that is as Cantor dimension increases the area of the spots represented the roughness becomes small and so the local pressure becomes higher, and also the surface becomes rougher.

7. Form figure (7.6) and (7.7) it can be noticed that as fractal dimension (D_f) decreases the difference in approach between the two Cantor dimensions becomes less, i.e. the difference in approach at the case D_f =1.24 is less than at D_f = 1.5.

8. As shown in figure (7.8)-figure (7.11), the agreement between the theoretical and experimental results (obtained by Handzel et.al (1991)) is good for the case of bead-blasted surfaces but for the case of turned surfaces

All Rights Reserved - Library of University of Jordan - Center of Thesis Deposit

www.manaraa.com

the agreement is not good because turned surface's properties is not constant and the roughness spots is not spread uniformly along the surface.

9. The agreement between the theoretical and experimental results is better as Cantor dimension increases because a more reality representation for the rough surface in this case.

Because of the periodicity of the Cantor set model it undergoes the same construction procedure at each hierarchical level producing contact areas that are all of the same size. Therefore, it is doubtful that this model will provide an exact simulation of the deformation of convex rough surface. However, the model does admit an analytic solution, and as proposed by Borodich and Mosolov (1992), it may in many cases be that:

(a) The specific character of a fractal model has little effect on the asymptotic behavior of the process, and

(b) The fractal dimension D_f that provides a measure of the rate at which a surface is changing is of most importance.

All Rights Reserved - Library of University of Jordan - Center of Thesis Deposit

www.manaraa.com

8.CONCLUSION AND RECOMMENDATIONS

Conclusion

Equation (6.16) obtained can be used to conduct exact analytic investigations of the solutions of contact problem of the convex punches regardless of their radius. But, nevertheless, it might turn out to be not too far from the reality, since tests on the actual contact area of polished (ground) metal surface show they contain sets of parallel ragged-edged scratches of different depths.

The solution obtained in this work provides further insight into the effect that surface structure has on the formation process, and it also provides indications of the effect that different surface finishing processes may have on subsequent surface deformation. Furthermore, in averaged sense the Cantor structure model appears to provide fairly reasonable results.

It has been also shown that fractal roughness of the convex punch surface of contacting bodies, gives the well –known power laws of the form $p \sim u^{\gamma}$.

It has been shown that the effect of bulk temperature on the relationship between the applied force and the approach is small which can be neglected, and if the contact problem is self-similar then its properties are independent of the choice of boundary conditions and valid for linear and nonlinear, isotropic and anisotropic media. So, we can say that the self-similar law of change of the solution is the general property of the considered problems. Cantor set surface has the advantage that it allows techniques known in mathematics, which are based on Euclidean geometry, to be applied to non-Euclidean geometry, since the element on which the technique is applied is Euclidean although the collection of elements is fractal.

All Rights Reserved - Library of University of Jordan - Center of Thesis Deposit

www.manaraa.com

Recommendations:

It is recommended to study the effect of friction in contact problems and reveal the relation between the roughness and the friction.

All Rights Reserved - Library of University of Jordan - Center of Thesis Deposit

www.manaraa.com

9. REFERENCES:

Abuzeid , O. M. 2002. Fractal Model of a Linear Thermoelastic Contact Between Flat Rough Surfaces Based on Cantor Structure. *Sixth International conference on production & design for development –PEDD6*, Cairo, february 12-14, 2002.

Abuzeid, O. M. 1997. Theoretical Analysis and Numerical Applications of the Contact Between Two Elastic Bodies Under Compression. *Ph.D. Thesis, Politecnico di Torino, Italy*

Abuzeid, O. M. 2002. A Linear Thermo-Visco-Elastic Creep Model for the Contact of Nominal Surfaces Based on Fractal Geometry :Kelvin-Voigt Medium.

Abuzeid, O. M. 2003. Linear Visco-Elastic Creep Model for the Contact of Nominal Surfaces Based on Fractal Geometry:Maxwell type medium. *Dirasat,engineering sciences, vol. 30, no. 1, 2003.*

Arthur, P. Boresi and Omar M. Sidebottom . Advance Mechanics of Materials. *4th edition.*

Bharat, Bhushan. 1996. Contact Mechanics of Rough Surfaces in Tribology :Single Asperity Contact. *app mech rev vol. 49, no 5.*

Borodich, F. M. and Mosolov, A. B. 1992. Fractal Roughness in Contact Problems. *Pergamon press Ltd-J. Appl. Maths Mechs 1992, Vol 56, No. 5 PP: 681-690, G.B.*

Borodich F. M. 1993. The Hertz Frictional Contact Between Nonlinear Elastic Anisottropic Bodies (the similarity approach). *Int. j . solids strectures vol. 30, no. 11 pp. 1512-1526.*

Borodich F. M. 1993. Similarity Properties of Discrete Contact Between a Fractal Punch and Elastic Medium. *Mechanics of solids, C. R. Acad. Sci . Paris, t.316, SerisII , PP. 281-286.*

All Rights Reserved - Library of University of Jordan - Center of Thesis Deposit

www.manaraa.com

Feder, Jens. 1988. Fractals. *2nd edition, Plenum press, New York- USA.*

Greenwood, J. A. and Tripp, J.H.1967. The Eastic Contact of Rough Spheres. *Journal of applied mechanics. March/153.*

Handzel, Z. T. and A. Polijaniuk. 1992. On the Experimental Verification of the Greenwood-Williamson model for the contact of rough surfaces. *Wear,154(1992)pp.115-124.*

Hearn, E. J. 1997. Mechanics of Matnials. *3rd ed. London, Britain.*

Hughes, J. R. and Marsden, E. Jerrold. 1983. Mathematical Foundations of Elasticity. *U.S.A.*

John, H. T. 1985. Hertzian Contact in Two and Three Dimension. *Nasa technical paper 2473.*

John, C. R. 1994. Fractal Surfaces. *plenum press, New york.*

Johnson, K. L.. 1985. Contact mechanics. *Cambridge University Press.*

Majumdar, A. and C. L.Tien. 1991. Fractal network model for contact conductance. *journal of heat transfer. 516 vol. 113, august 1991.*

Meguid, S. A….et.el, 2001. Numerical and Experimental Studies of Multiple Discs in Contact. *International journal of computational engineering science, vol. 2,no. 1,pp. 75-93.*

Miroslav, M. Novak.1995. Fractal Reviews in the Natural and Applied Sciences. *published by chapman &hall.*

Panagiotopoulos, P. D. 1991. Fractal Geometry in Solids and Structures. *Int.j. solids structures vol. 29, no. 17, pp . 2159-2175.*

Panagiotopoulos, P. D. and O. K. panagouli . 1994. Numerical Methodes for Convex Energy Problems. *Int. j. solids structures vol. 31, no. 16, pp . 2211-2228.*

All Rights Reserved - Library of University of Jordan - Center of Thesis Deposit

www.manaraa.com

Panagiotopoulos, P. D. et. al. 1993. Fractal Geometry and Fractal Material Behaviour in Solids and Structures. *Archive of applied mechanics 63 . pp 1-24.*

Robert, C. W. Handbook of Tables for Mathmatics. *4th edition , published by the chemical rubber co.*

Robert, D. Cook and Warren C. Young .1985. Advanced Mechanics of Materials. *Macwillam publishing Co. –U.S.A.*

Rubtsov, V. E. et. al. 1998, Study of the Formation of Contact Between Rough Surfaces on the Particle Method. *Technical physics letters, vol . 24, no. 3.*

Stefan, B. 2001. The Influence of Surface Roughness in Elliptical Contacts. *tribology international 34, pp. 841-845.*

Takayasu, H. 1990. Fractals in the Physical Sciences. *Manchester university press.*

Takayasu, H. 1990. Fractals in the physical science. *New York USA.*

Thomas, L. W. and Dusan Krajcinovic. 1995. Fractal Models of Elastic-Perfectly Plastic Contact of Rough Surfaces Based on the Cantor Set. *Pergamon press Ltd, International Journal of solids structure, 1995, Vol. 32, No. 19, PP: 2907-2922, G.B.*

Warren, T. L. , Majumdar and Krajcinovic, D. 1996. A Fractal Model for the Rigid Perfectly Plastic of Rough Surfaces . *Vol. 63, Journal of Applied Mechanics, pp: 47-54, U.S.A.*

Woo, k. l. and thomas, T.R. 1980. Contact of rough surfaces :areview of experimental work. *Wear , 58, pp. 331-340.*

Yan, W. and Komvopoulos, K.1988. Contact Analysis of Elastic-Plastic Fractal Surfaces. *Vol . 84, No. 7, Journal of Applied Physics, Calfornia –U.S.A, PP:3617-3624.*

All Rights Reserved - Library of University of Jordan - Center of Thesis Deposit

www.manaraa.com

Aappendix A

Figure (A.1) two gears in mesh

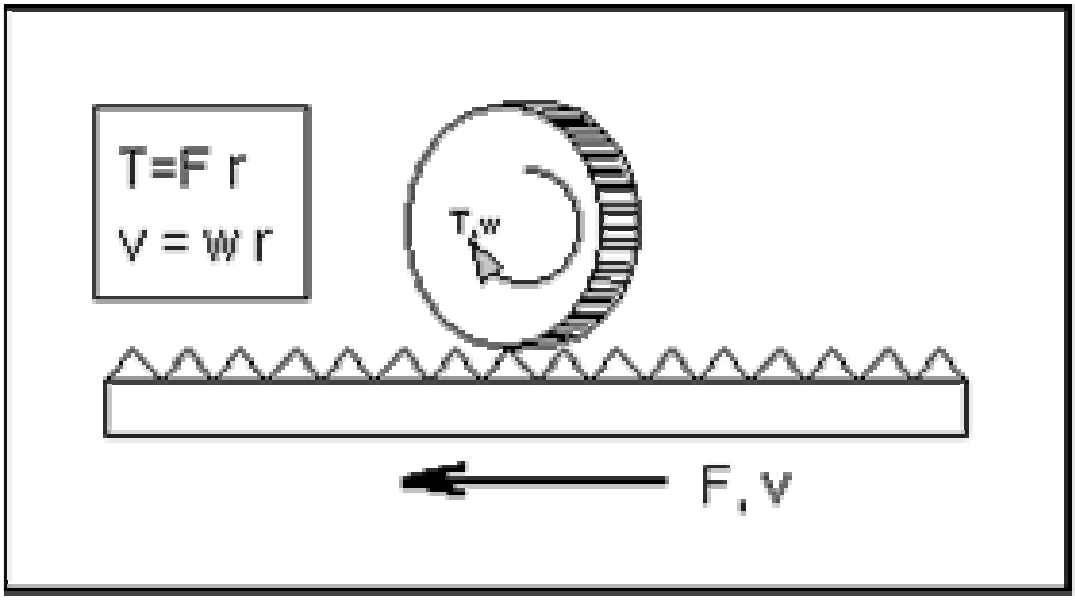

Figure (A.2)

All Rights Reserved - Library of University of Jordan - Center of Thesis Deposit

www.manaraa.com

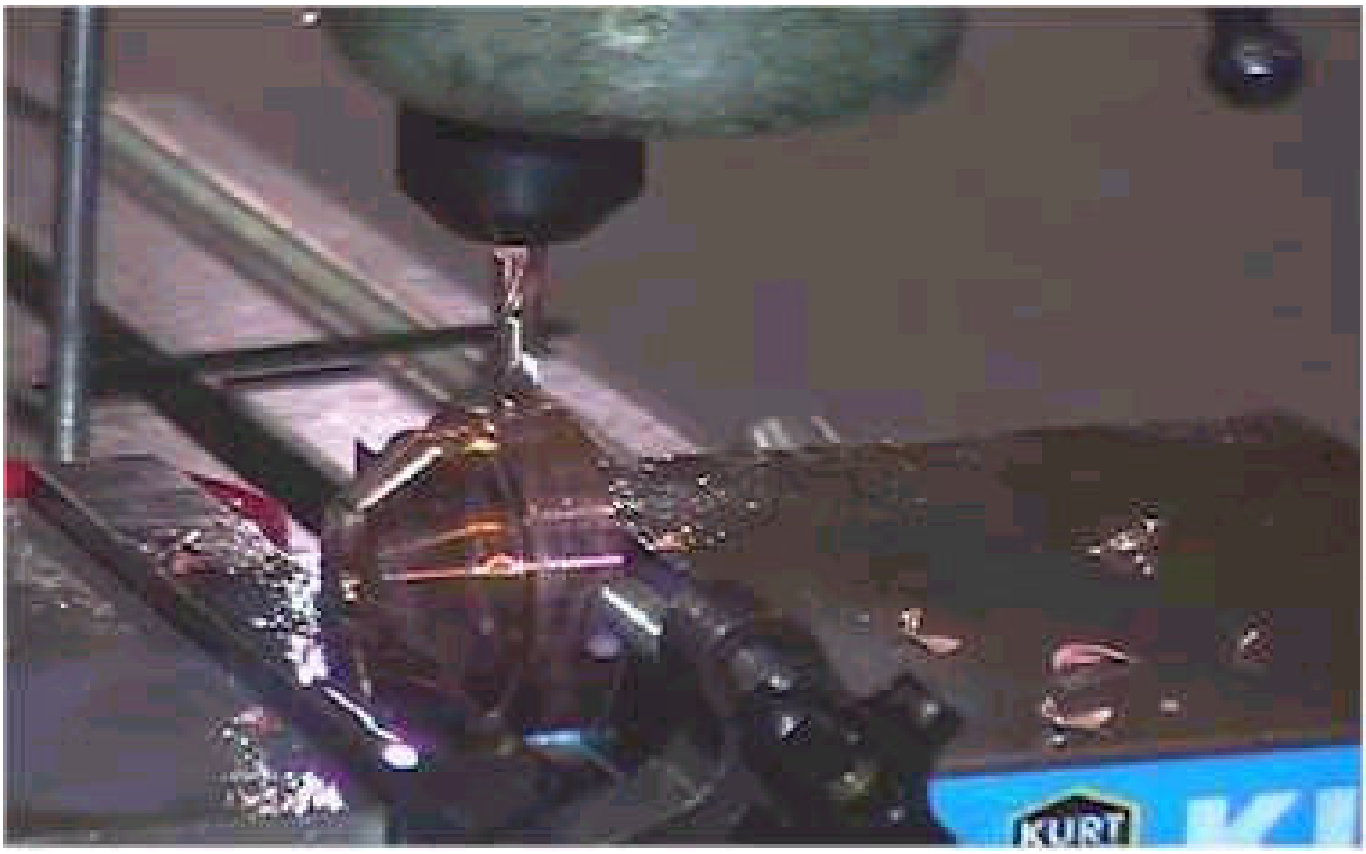

Figure (A.3) spot welding operation

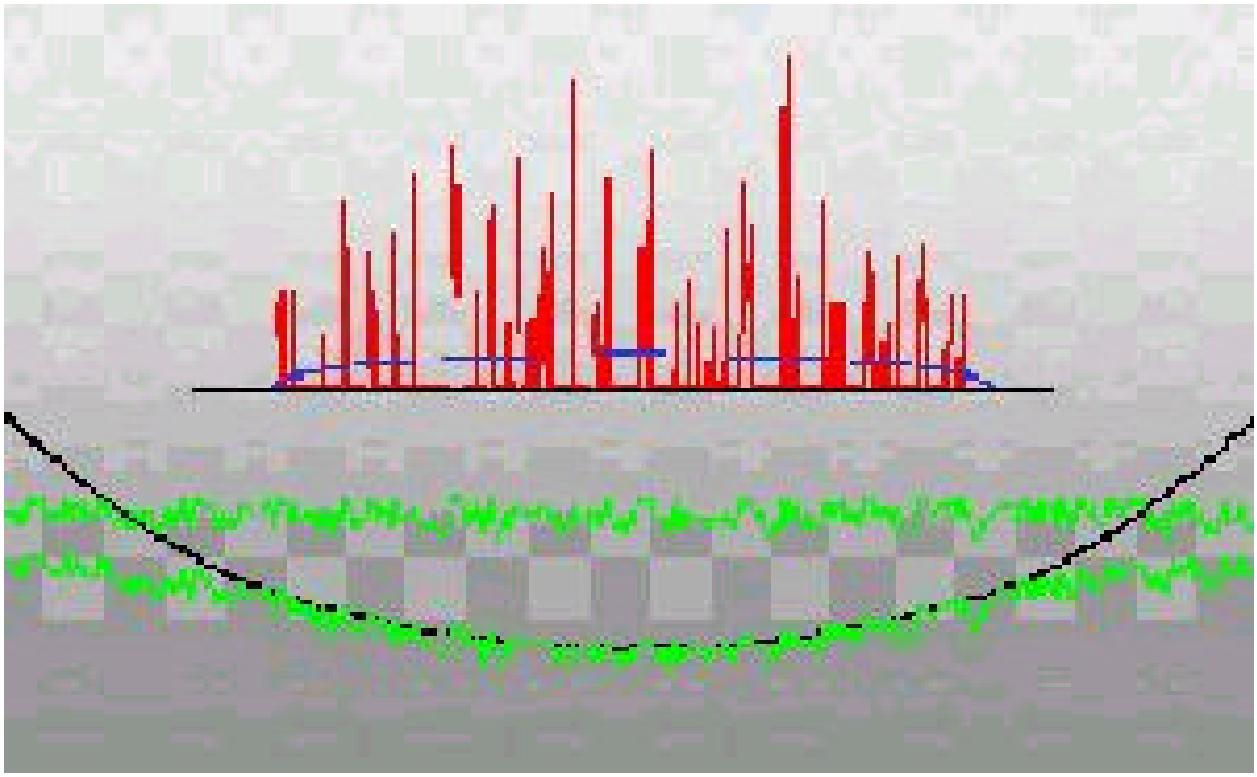

Figure (A.4) a simulation represents the rough punch

All Rights Reserved - Library of University of Jordan - Center of Thesis Deposit

المنارة للاستشارات
www.manaraa.com

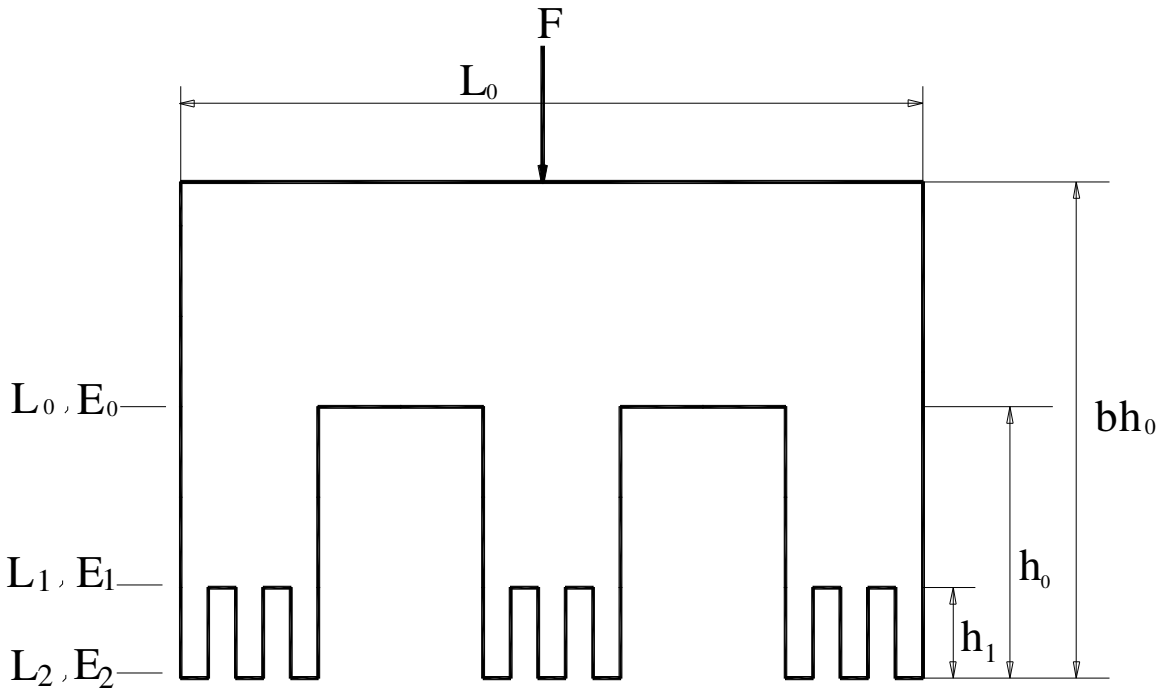

Figure (5.2) Cantor structure, s=3, Dc=0.6228.

All Rights Reserved - Library of University of Jordan - Center of Thesis Deposit

www.manaraa.com

"نموذج حراري مرن لدراسة سلوك مكبس محدب خشن يتلامس مع جسم آخر باستخدام الهندسة غيرالاقليدية (الفراكتال) "

اعداد
صايل محمد علي فياض

المشرف

الدكتور اسامة محمود ابو زيد

ملخص

تعتبر الاجهادات الناتجة عن عمليات التلامس (Contact) بين الأجسام المختلفة ذات أهمية كبيرة ذلك أنها تسبب في كثير من الأحيان إلى حدوث تشققات(Cracks) في الأجسام المتلامسة تلك التشققات التي قد تؤدي إلى انهيار محتمل للمادة تحت الإجهاد .

في هذا البحث تم دراسة التلامس(Contact) بين مكبس محدب(Convex) خشن(Rough) وجسم آخر اعتبر صلب (Rigid) بطريقة الهندسة غير الاقليدية (غير المستوية) أو ما يسمى الفراكتل(Fractal) لقد تم اشتقاق علاقة جديدة بين القوة المؤثرة(Applied force) والتشوه (Deformation) وذلك بالاعتماد على الفراكتال ومجموعة كانتور(Cantor set) .لقد وجد أن علاقة القوة المؤثرة (P) بالتشوه (u) تمثلت بالعلاقة ($p \sim u^{\gamma}$). إن مقارنة النتائج التي تم الحصول عليها من رسم هذه العلاقة والنتائج العملية قد اظهر توافقا جيدا . لقد ظهر جليا تأثير البعد الخاص بالسطح الخشن (Fractal dimension) في النتائج .

All Rights Reserved - Library of University of Jordan - Center of Thesis Deposit

المنارة للاستشارات
www.manaraa.com